Supplementary information

Optimising the structure of mesoporous niobium oxide using evaporation-induced self-assembly synthesis method

Peter Nadrah[1], Mateja Knap[1], Erika Švara Fabjan[1], Andraž Šuligoj[2,3], Urška Lavrenčič Štangar[2], Goran Dražić[3], Nataša Novak Tušar[3,4] and Andrijana Sever Škapin[1,5]

1 Slovenian National Building and Civil Engineering Institute, Dimičeva ulica 12, 1000 Ljubljana, Slovenia
2 University of Ljubljana, Faculty of Chemistry and Chemical Technology, Večna pot 113, 1000 Ljubljana, Slovenia
3 National Institute of Chemistry, Hajdrihova ulica 19, 1000 Ljubljana, Slovenia
4 University of Nova Gorica, Vipavska cesta 13, 5000 Nova Gorica, Slovenia
5 Faculty of Polymer Technology, Ozare 19, 2380 Slovenj Gradec, Slovenia

Contents

Acid site concentration

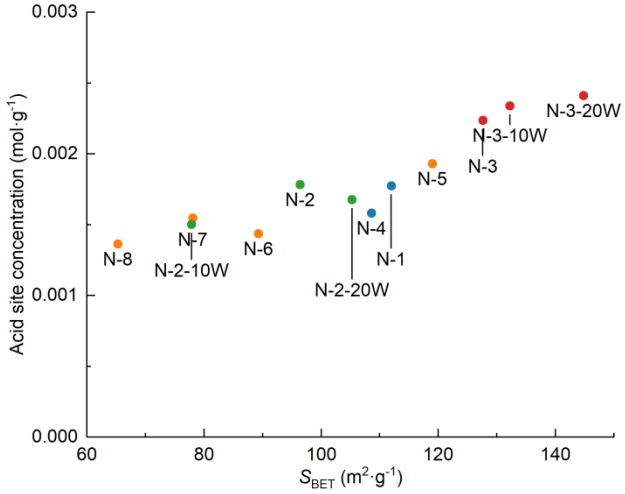

Figure S1. Acid site concentration vs. S_{BET}.

High-angle X-ray diffraction

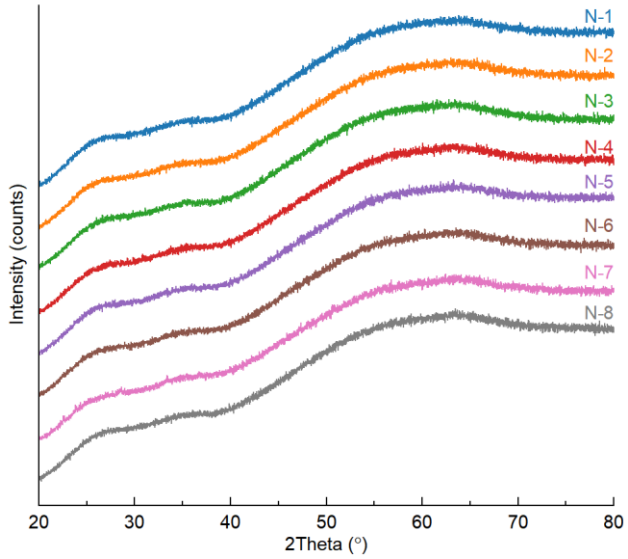

Figure S2. High-angle diffractograms of N-1 through N-8. Curves are offset on the y-axis.

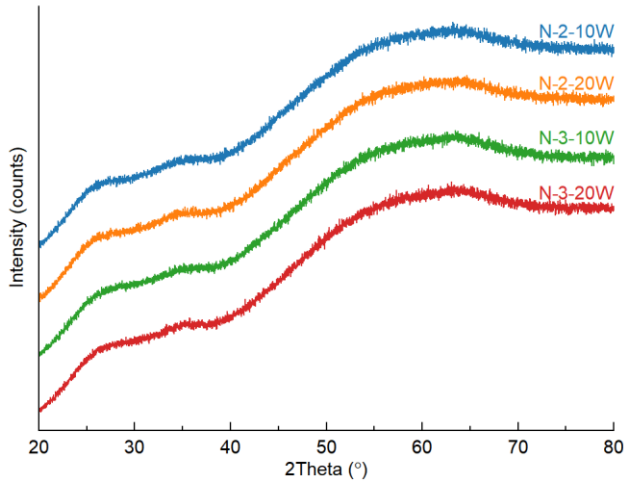

Figure S3. High-angle diffractograms of additional N-2 and N-3 samples. Curves are offset on the y-axis.

Transmission electron microscopy

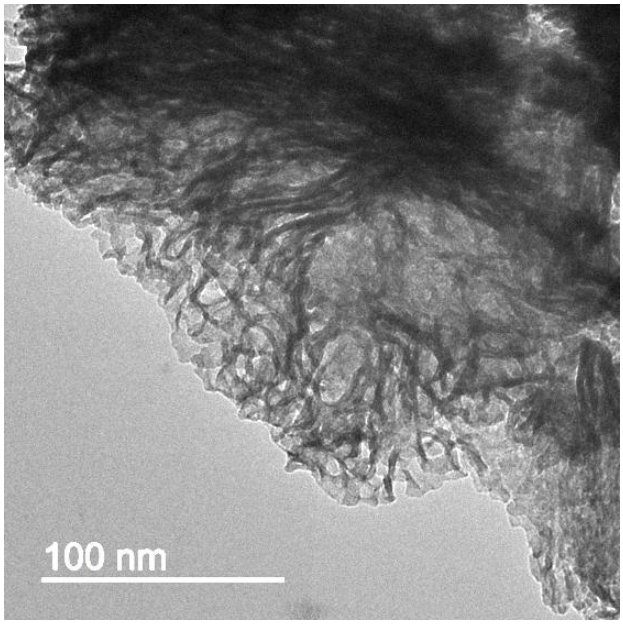

Figure S4. TEM micrographs of N-7. Unordered pores of various sizes can be seen in the centre.

X-ray photoelectron spectroscopy

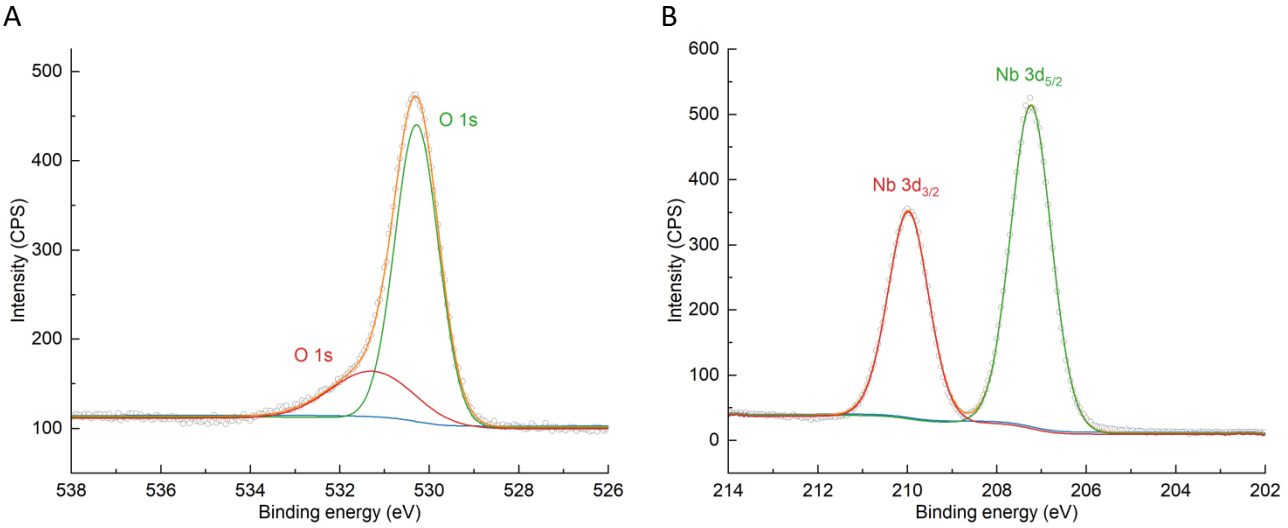

Figure S5. XPS spectra of O 1s (A) and Nb 3d (B) of N-2 sample.

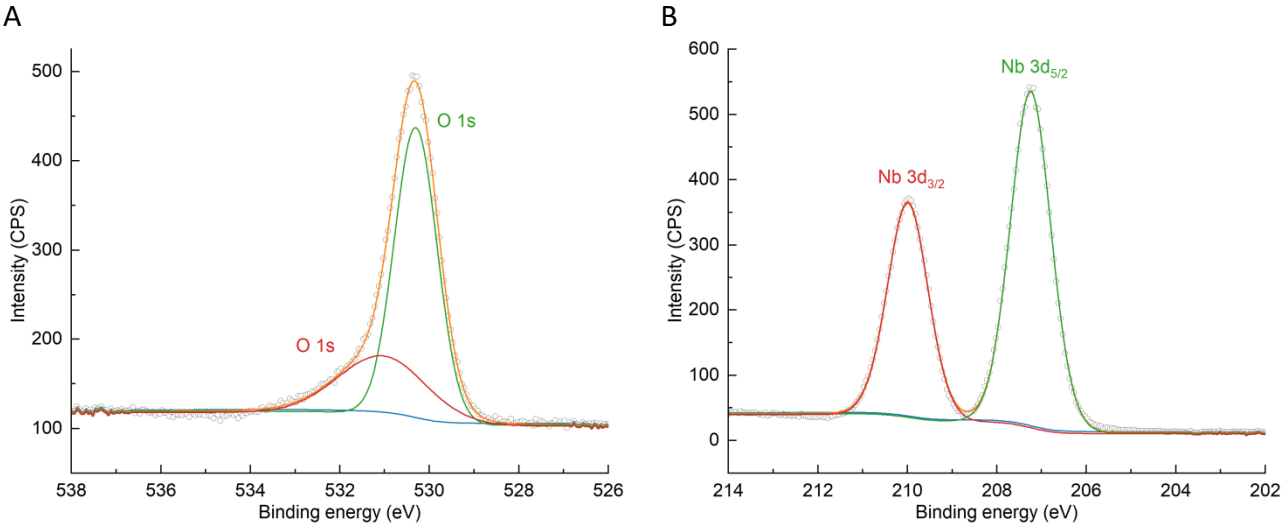

Figure S6. XPS spectra of O 1s (A) and Nb 3d (B) of N-3 sample.

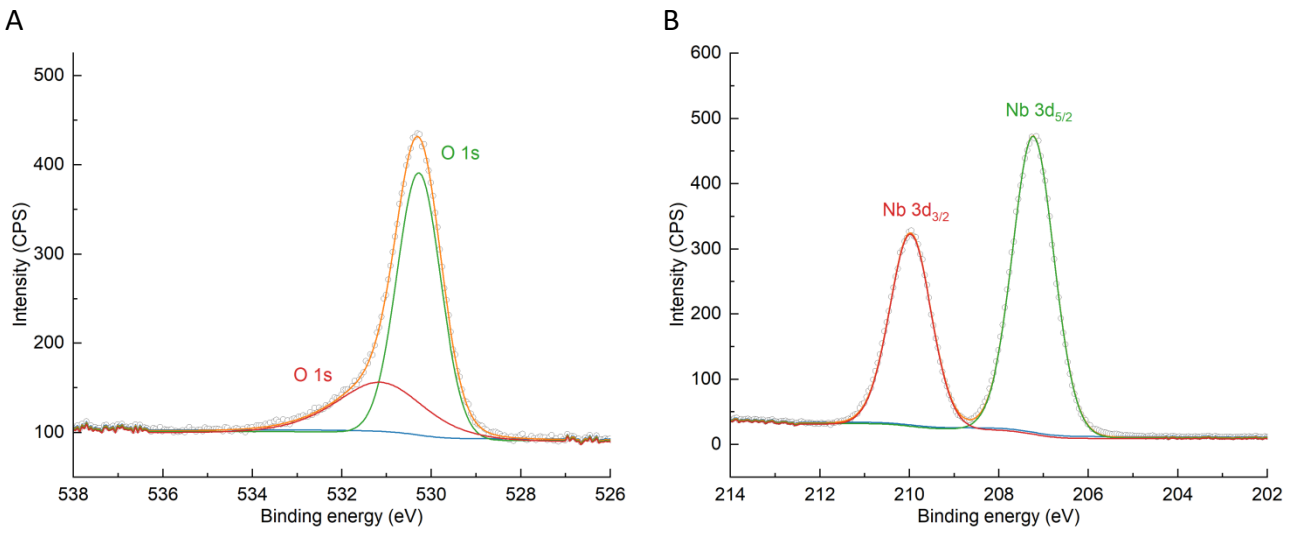

Figure S7. XPS spectra of O 1s (A) and Nb 3d (B) of N-6 sample.

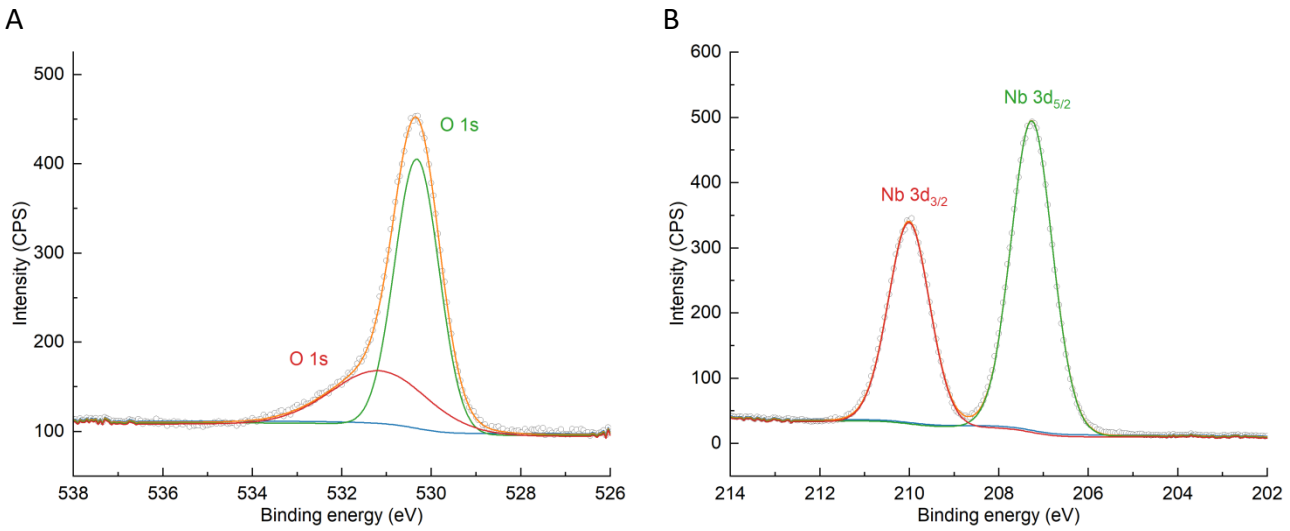

Figure S8. XPS spectra of O 1s (A) and Nb 3d (B) of N-7 sample.

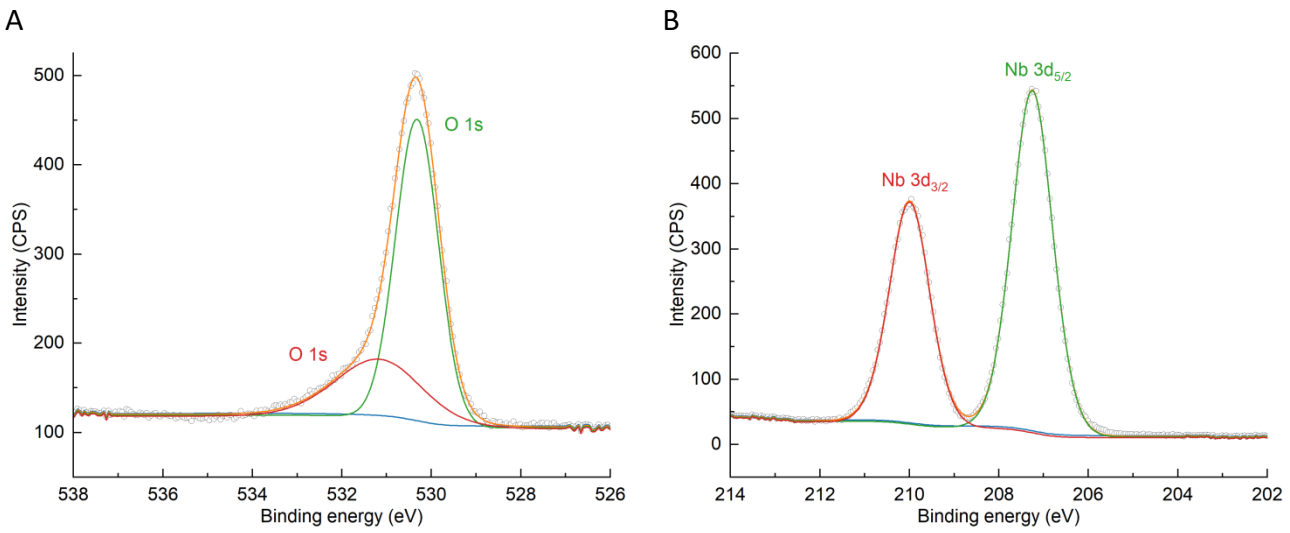

Figure S9. XPS spectra of O 1s (A) and Nb 3d (B) of N-3-10W sample.

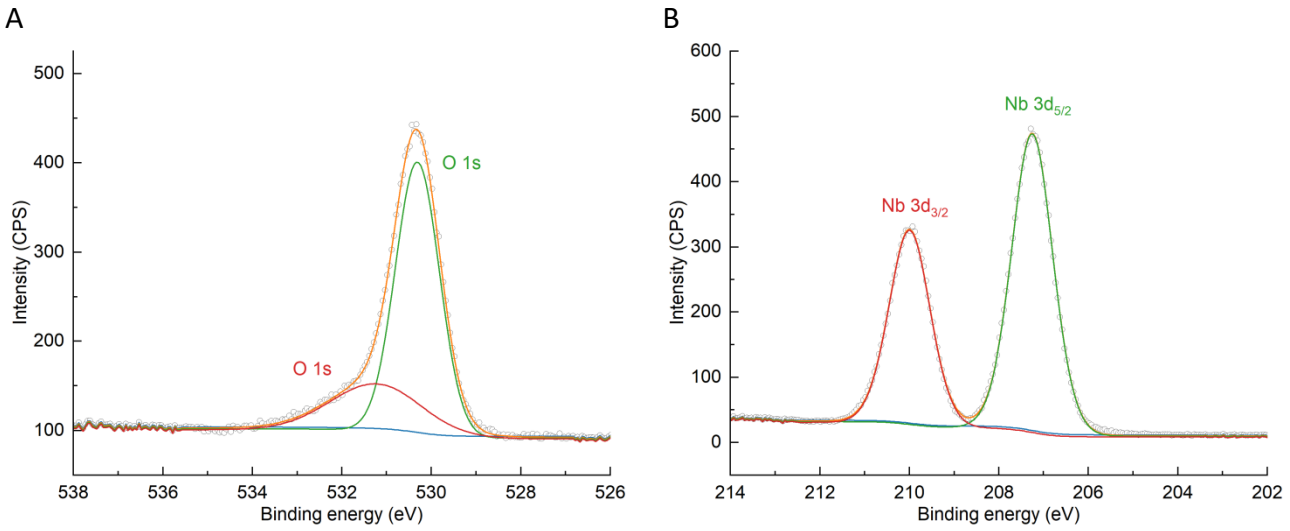

Figure S10. XPS spectra of O 1s (A) and Nb 3d (B) of N-3-20W sample.

Table S1. Nb:O and $O_{surface}$:$O_{lattice}$ ratios calculated from Nb 3d and O 1s peaks.

material	Nb:O ratio (%)	$O_{surface}$:$O_{lattice}$ ratio (%)
N-2	33:67	24:76
N-3	34:66	22:78
N-3-10W	33:67	23:77
N-3-20W	34:66	21:79
N-6	34:66	23:77
N-7	32:68	22:78

Fourier-transform infrared spectroscopy

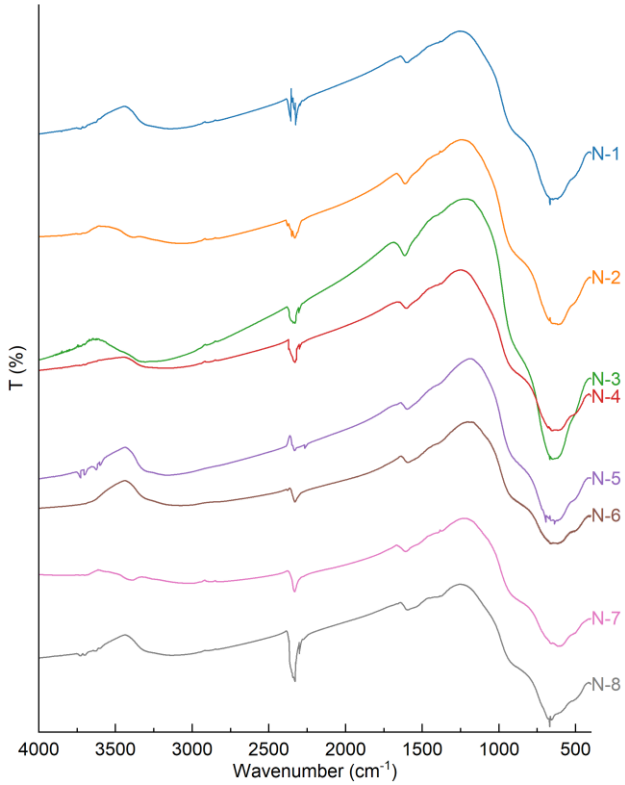

Figure S11. FTIR spectra of N-1 through N-8. Spectra are offset on the y-axis.

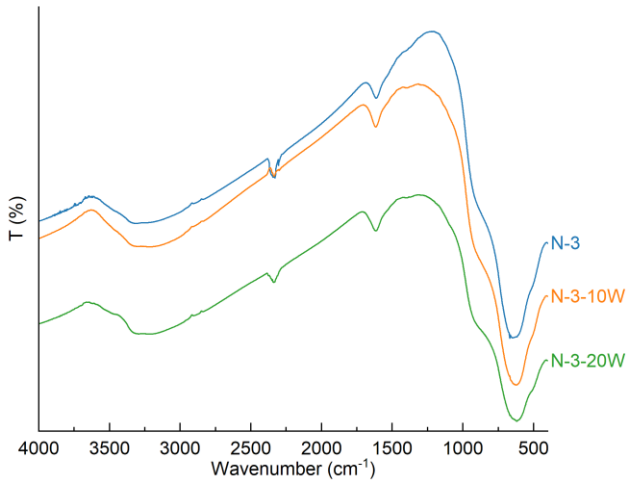

Figure S12. FTIR spectra of N-3-10W and N-3-20W. Spectra are offset on the y-axis.

Diffuse reflectance spectroscopy

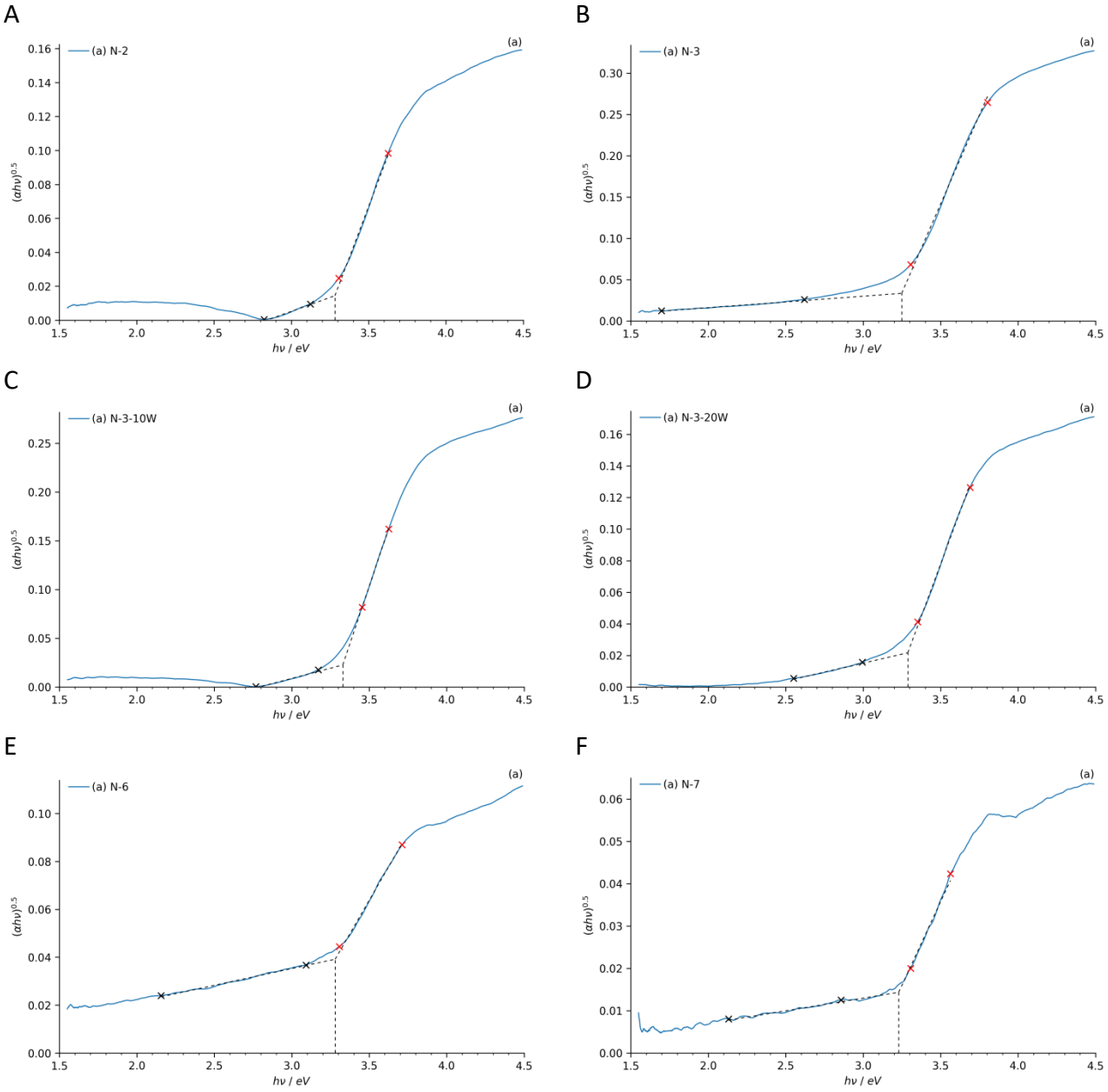

Figure S13. Tauc plots of the selected samples for calculating the band gaps of the materials: (A) N-2, (B) N-3, (C) N-3-10W, (D) N-3-20W, (E) N-6 and (F) N-7.

Table S2. Band gap energies of the selected materials.

material	Band gap energy (eV)
N-2	3.28
N-3	3.25
N-3-10W	3.33
N-3-20W	3.29
N-6	3.28
N-7	3.23

Energy dispersive X-ray spectroscopy

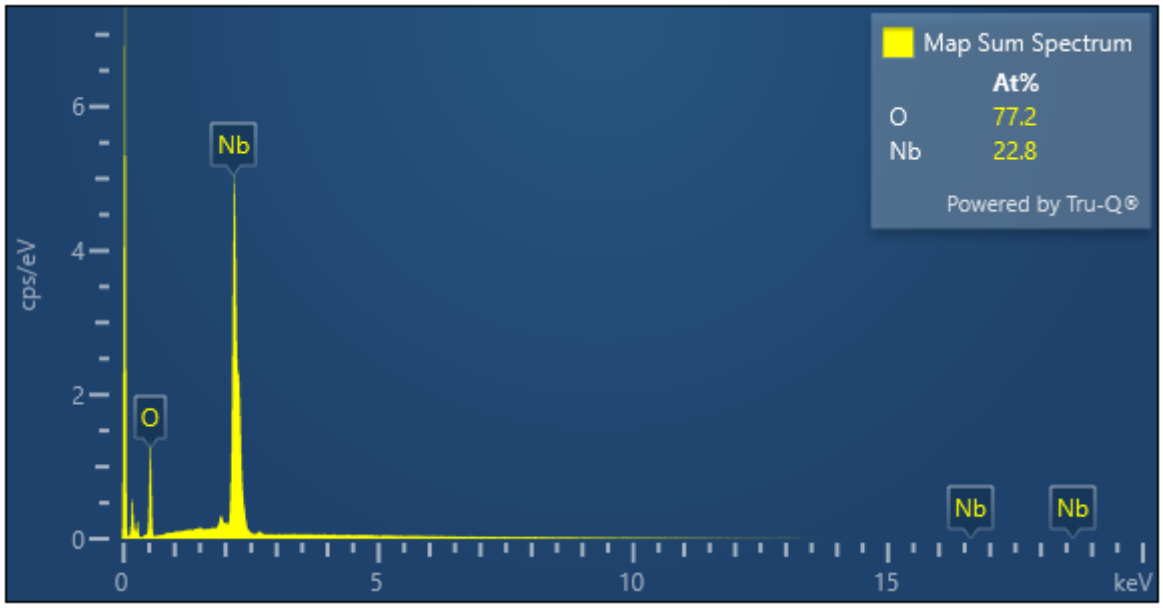

Figure S14. EDS mapping for N-3-20W.

Photocatalytic measurements

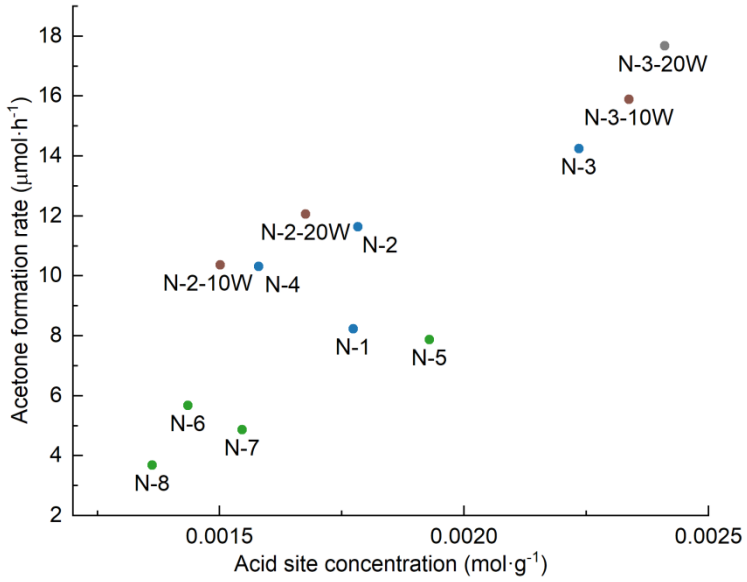

Figure S15. Activity vs. acid site concentration.

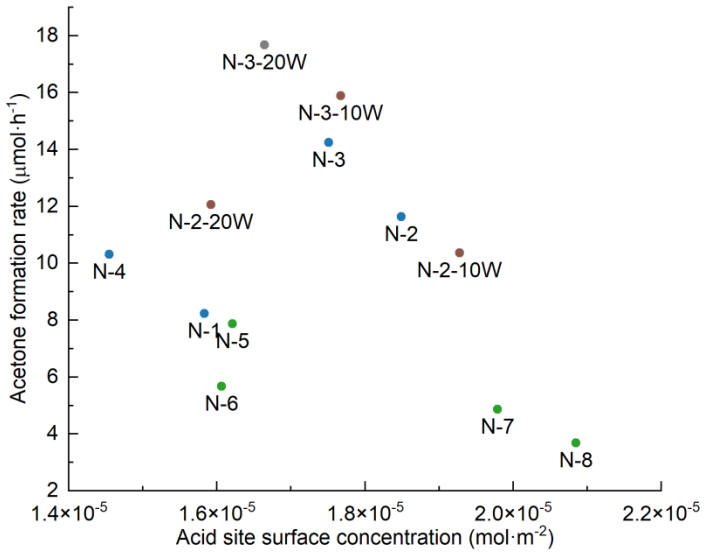

Figure S16. Activity vs. acid site concentration per unit surface area.

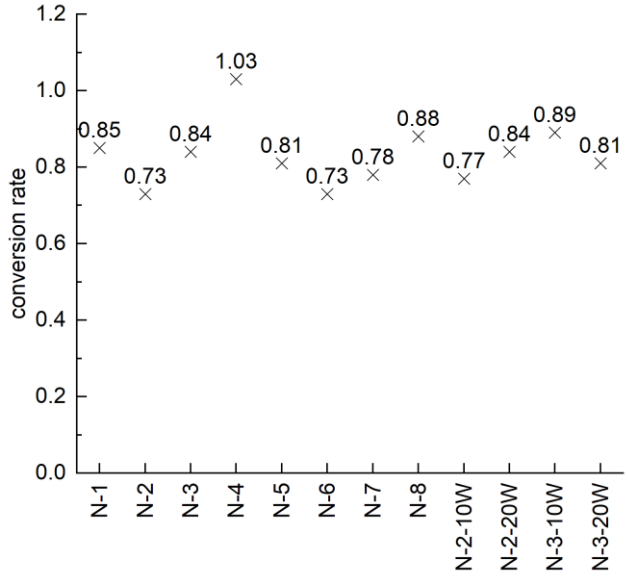

Figure S17. Conversion rates of isopropanol into acetone under UV light.

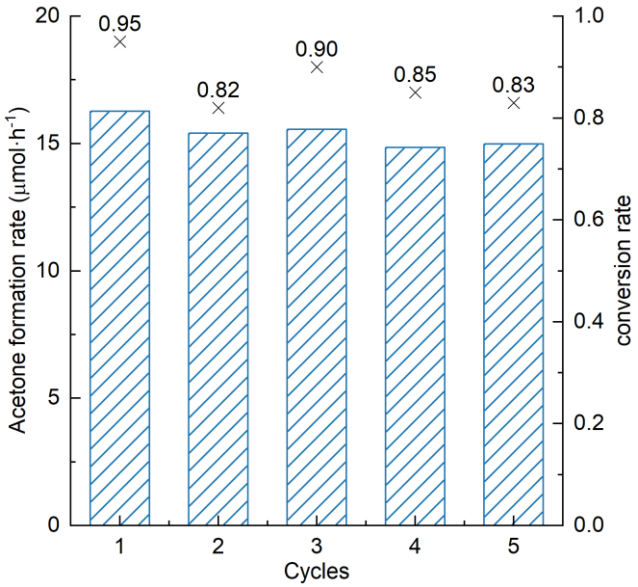

Figure S18. Stability data (bars) and conversion rates (markers) of the N-3-20W over 5 consecutive cycles.

Nitrogen sorption after photocatalytic reaction

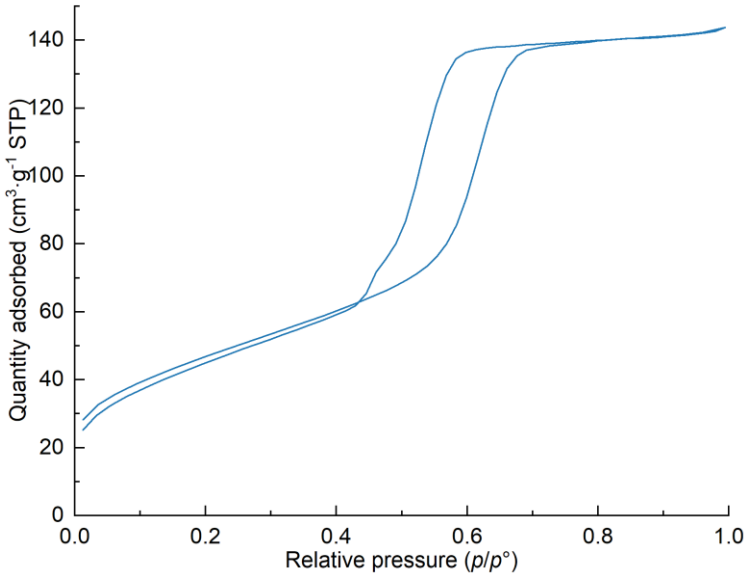

Figure S19. Nitrogen sorption isotherm for N-3-20W after 5 cycles of photocatalytic reactions.

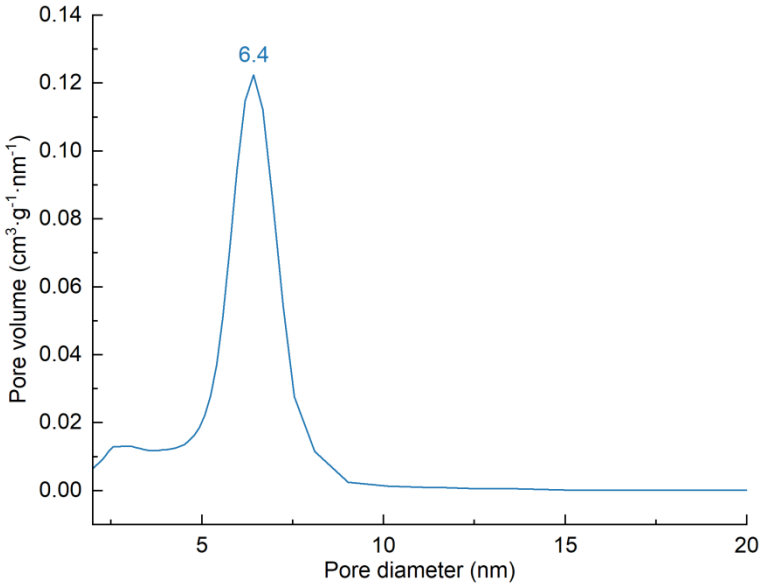

Figure S20. Pore size distribution for N-3-20W after 5 cycles of photocatalytic reactions. Peak is marked with a pore diameter value in nm at the maximum height.

Photographs

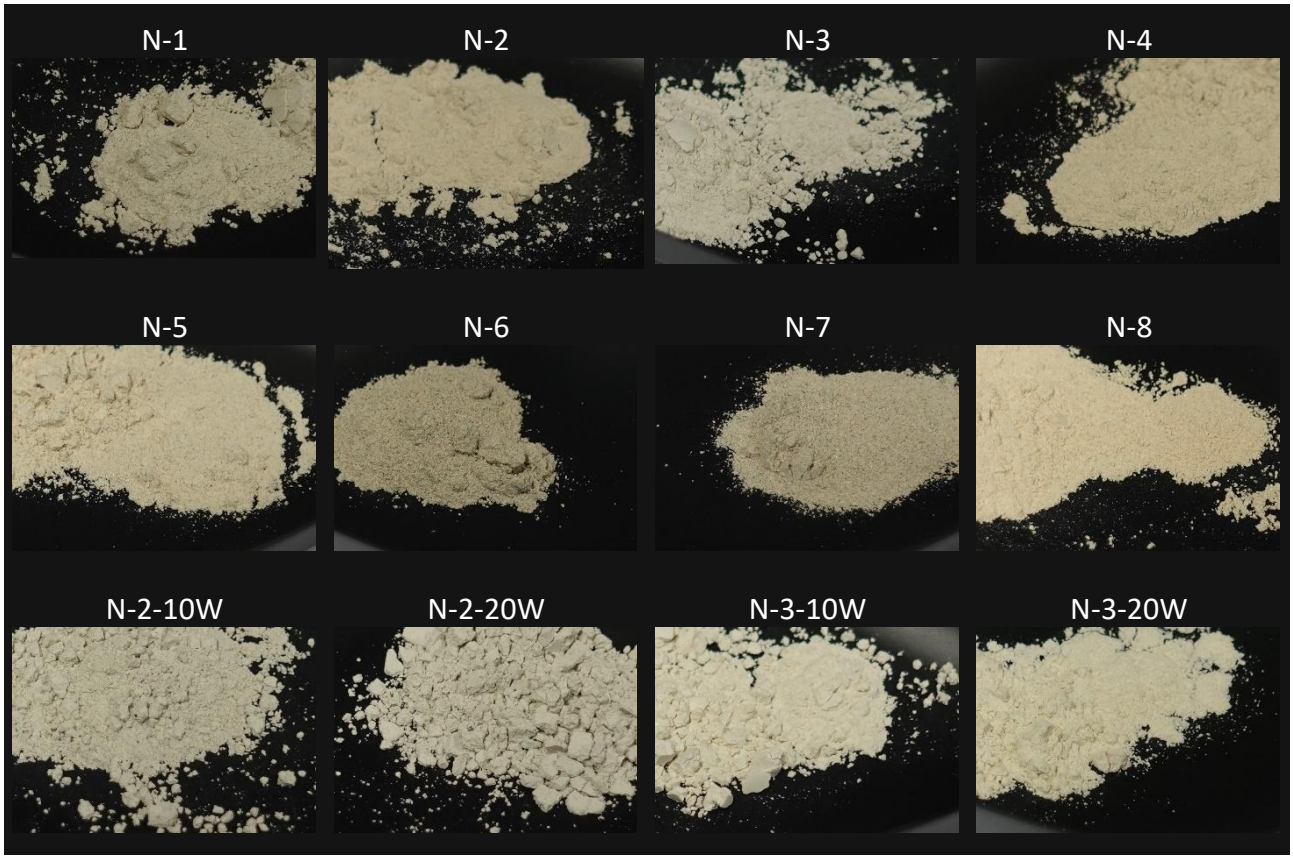

Figure S21. Photographs of the materials.